JOURNAL OF MATERIALS SCIENCE 15 (1980) 3017–3024

The effect of MgO additions on the kinetics of hot pressing in Al_2O_3

M. P. HARMER, R. J. BROOK
Department of Ceramics, University of Leeds, Leeds, UK

The kinetics of hot pressing of Al_2O_3 with and without MgO additives have been measured at 1475 and 1630° C and at 5 to 20 MPa using Al_2O_3 powders of different grain size and using different additive levels. Data obtained within the solid solution regime are interpreted in terms of diffusional creep processes. MgO additions accelerate densification within this regime; the consequent reduction in pore size, and hence in pore drag, can explain the function of MgO as sintering additive for Al_2O_3.

1. Introduction

Through the use of additives, many ceramics [1] can now be sintered to theoretical density. Unfortunately, the choice of a suitable additive remains largely empirical primarily because of the widespread disagreement that still exists concerning the specific function of additives. A classic example in this respect is the case of MgO-doped Al_2O_3. Although some twenty years have elapsed since Coble [2] discovered that a small amount of MgO prevents the onset of abnormal grain growth in Al_2O_3 (this striking effect is illustrated in Figs 1 and 2), the operative mechanism remains a strongly debated issue [3].

Some important factors contributing to the difficulty of understanding how an additive works are discussed below.

1.1. The possibility of multiple roles

There is a wide range of possible roles to choose from. In solid solution an additive may:

(a) Alter diffusion coefficients by modifying point defect concentrations [5].

(b) Inhibit boundary migration by a solute drag mechanism [6].

(c) Alter the surface energy/boundary energy ratio and influence the driving force for densification [7] and pore morphologies [8].

(d) Assist in sintering by easing the emission and absorption of point defects at grain boundaries where interface reactions are important [9].

As a second phase at the boundary an additive may:

(1) Provide high diffusivity paths [10].

(2) Inhibit boundary migration by pinning [11].

Precise identification of the operative mechanism is further complicated by the fact that an additive may operate by a combination of these mechanisms. This occurrence of different mechanisms under different experimental conditions, for example, of grain size or temperature, can explain many of the contradictory findings reported in the literature. Peelen [4] has demonstrated two modes of operation for MgO in Al_2O_3 depending on the MgO content; his work provides a clear demonstration of the need, in the first instance, to separate effects due to second phases and those caused by impurity solutes alone.

1.2. Problems associated with characterization

The small amounts of additive used in sintering can make microstructural identification of the additive a very difficult task. Standard methods such as X-ray diffraction and optical microscopy are often not good enough in terms of both the resolution required and detection limits involved. As a consequence the presence of second phases can, for example, go unnoticed. Furthermore, uncertainties can occur when indirect measurements techniques such as microhardness are used [12]. To overcome these problems, some attention has been given to surface analysis techniques such as Auger electron spectroscopy [13] and to high resolution electron microscopy using techniques such as lattice fringe imaging [14].

0022–2461/80/123017–08$02.80/0

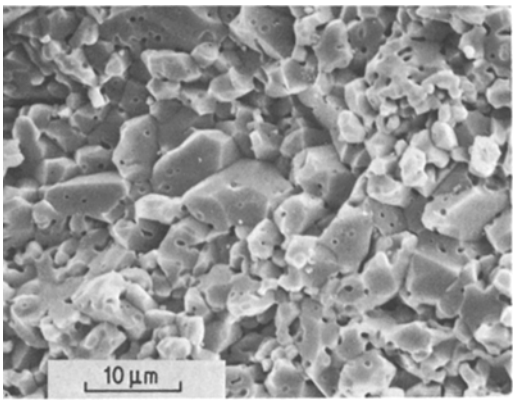

Figure 1 Scanning electron micrograph of Al_2O_3 sintered without additive.

Even then, uncertainties remain and the merit of using a range of different techniques has been recognized.

1.3. Identification of the rate controlling sintering mechanism

The behaviour of an additive during sintering cannot be properly identified unless the rate controlling mechanism responsible for densification is known. This in itself can present a substantial problem, the difficulties being: (a) the occurrence of processes which may interfere with and impede densification, such as surface diffusion and grain growth; (b) the diversity of possible densification mechanisms and transport paths; (c) the complex geometries of real powder compacts; and (d) the lack of reliable supporting data such as diffusion coefficients.

All of these complexities make it difficult to design experiments from which convincing conclusions may be drawn concerning the role of an additive. One obvious solution to this problem is to try to minimize the complexity. This may be done by (i) working on simplified and well controlled microstructures (particularly in terms of the presence or absence of second phases) and (ii) by designing the experimental conditions to favour the process of interest, in this case densification, so that it predominates over interfering processes such as surface diffusion and grain growth.

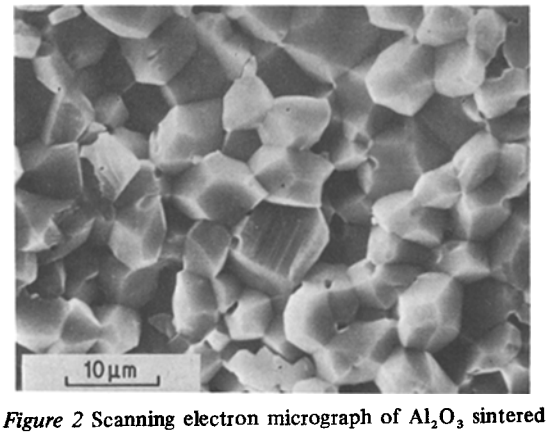

Figure 2 Scanning electron micrograph of Al_2O_3 sintered with 200 ppm MgO as additive.

Enhancement of densification can be achieved by two methods. The first is hot pressing in which external pressure is used to increase the driving force for densification without substantially altering the driving forces for surface diffusion or grain growth. This technique is now showing considerable promise for isolating and identifying single controlling mechanisms [15]. The second method is to use zone sintering [16] developed specifically for the fabrication of β-alumina ceramics. In this process the sample is sintered for a short time at a very high temperature. The resulting enhancement of densification is believed to stem from the generally higher activation enthalpies of densification mechanisms (such as lattice and grain boundary diffusion) as compared with the enthalpies of the surface diffusion mechanisms often responsible for the rival processes.

In other papers [17, 18] we have reported our findings on the behaviour of MgO in the zone process and a qualitative model to account for the role of the additives has been advanced. The purpose of the present work has been to study the hot pressing behaviour of Al_2O_3, pure and doped with increasing amounts of MgO, with the objective of quantifying the earlier findings concerning the role of the additive, and of clarifying the atomic mechanisms responsible for densification in Al_2O_3.

2. Experimental procedure

2.1. Powder preparation

Small grain size powders (0.3 μm) were prepared from high purity Linde A alpha alumina powders. Larger grain size powders (3, 7 and 10 μm) were prepared by classifying a coarser grade alumina powder (Analar grade) into the required particle size fractions using a Zig-Zag particle size classifier (Alpine Ltd.). Iron impurity was unavoidably introduced into the powders during classification and was subsequently removed (to 10 ppm,

checked by atomic absorption) by dissolving in a hot acid solution (50:50 $HCl:HNO_3$) for 48 h followed by repeated filter washing in distilled water.

Magnesium-doped alumina was prepared by mixing an alcohol solution of $Mg(NO_3)_2$ (Analar grade) into a slurry with the alumina and evaporating off the alcohol under an infra-red lamp while stirring continuously. Each batch was calcined at 600° C to decompose the nitrate and sieved afterwards to break down agglomerates.

2.2. Hot pressing procedure

The hot press and its ancillary equipment are described fully elsewhere [19]. Specimens were hot pressed in high purity graphite dies (nuclear grade) with either a 2.5 or a 1.25 cm bore diameter using high density graphite punches. The inner die walls and the contact surfaces of the graphite punches were coated with a thin layer of boron nitride powder to prevent the alumina from reacting with the graphite. Equal amounts of powder were used for each hot pressing (7 g for the 2.5 cm die and 2.5 g for the 1.25 cm die). The hot-pressing procedure was identical to that used by Bowen *et al.* [20]. Shrinkage of the sample was monitored continuously throughout sintering. The final density and thickness of the hot-pressed discs were measured to compute the density–time curves from the displacement data. Densities were measured by water immersion or mercury immersion for high or low density specimens respectively.

3. Results

Densification rates were measured as a function of the three process variables: applied pressure, grain size and MgO content. Measured rates were obtained at constant values of relative density (usually 0.85, although 0.75 was used for low densification rates) by measuring the slopes of the tangents drawn to the density–time curves at the appropriate density values. The advantages of taking measurements during the late intermediate stage of sintering are (i) that relative densities of 0.85 and 0.75 should be well beyond those where densification by particle rearrangement is still important [15], (ii) that the differences between the alternative suggestions for a stress concentration factor [21, 22] are not so important at this stage of sintering and (iii) that the surface energy contribution to the total driving force is minimal in the intermediate stage [23].

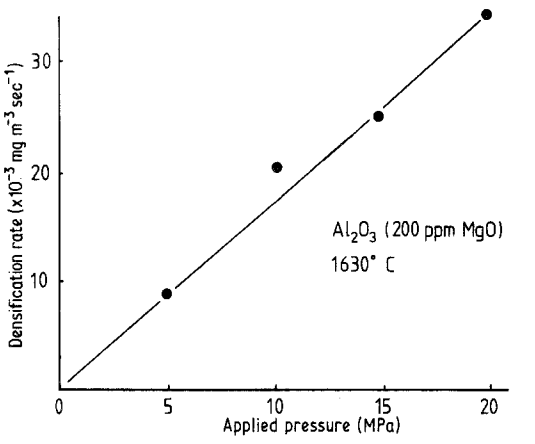

Figure 3 Pressure dependence of the densification rate in doped Al_2O_3.

3.1. Dependence of the densification rate on pressure

The dependence of the densification rate (at 0.85 relative density, 1630° C) on applied pressure for Al_2O_3 doped with 200 ppm MgO is shown in Fig. 3. (This additive level is below the solubility limit [24] at the temperature used.) The data show an approximately linear dependence of densification rate on applied stress.

3.2. Dependence of the densification rate on grain size

The dependence of densification rate on grain size was measured for three sets of experimental conditions, namely for pure and for MgO-doped (200 ppm) Al_2O_3 at 1630° C (0.85 relative density) and for pure Al_2O_3 at 1475° C (0.75 relative density). The low temperature data (Fig. 4) for pure Al_2O_3 indicate a proportionality between densification rate and $(\text{grain size})^{-2}$. At the higher temperature of 1630° C, the data for pure and for MgO-doped Al_2O_3 indicate mixed behaviour with a shift in the grain size exponent from -2 at small grain sizes to -3 at larger grain sizes. The MgO-doped material densifies noticeably more quickly than the pure materials in the smaller grain size range.

3.3. Dependence of densification rate on MgO content

Data showing the dependence of the densification rate (0.85 relative density) on the MgO content over a wide range of additive levels starting from below the theoretical [24] solid solution limit

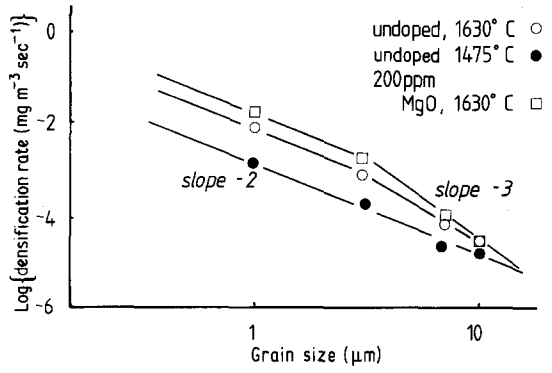

Figure 4 Grain size dependence of the densification rate of pure and MgO-doped aluminas.

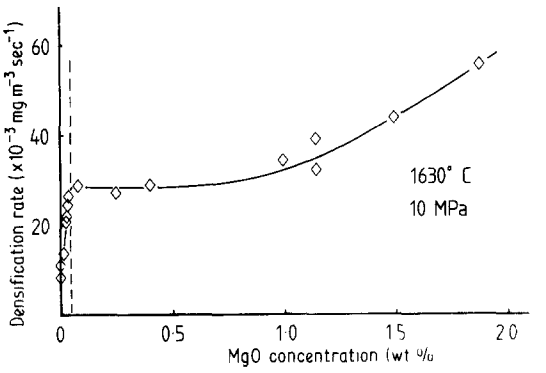

Figure 6 Dependence of the densification rate of Al_2O_3 on the MgO content showing enhanced densification in both the solid solution regime and the second phase regime at high dopant levels (possibly due to enhanced diffusivity within the second phase particles).

(~ 250 ppm at 1630° C) are shown in Figs 5 and 6. Inspection of the data shows that, at very low additive concentrations (up to ~ 400 ppm MgO), a linear increase in densification rate with MgO content is observed. At higher dopant levels, saturation occurs and the rate levels off. At very high MgO concentrations (≳ 1 wt%), a further increase in rate with MgO content is observed.

4. Discussion

4.1. Interpretation of the hot pressing data

4.1.1. Pressure dependence

The observation of a stress exponent of approximately unity suggests that a diffusional creep mechanism is responsible for densification [25, 26]. The results may therefore be usefully interpreted in terms of one of the diffusional creep models suitably modified for hot pressing [27]. The two pertinent models relate the densification rate to the effective stress (σ_{eff}) on the particles by the equations

$$\frac{1}{\rho}\frac{d\rho}{dt} = \frac{40 D_L \Omega}{3kT(G)^2}\sigma_{eff}, \qquad (1)$$

corresponding to conditions where the diffusion step is through the lattice (Nabarro–Herring creep), and

$$\frac{1}{\rho}\frac{d\rho}{dt} = \frac{47 \delta D_b \Omega}{kT(G)^3}\sigma_{eff}, \qquad (2)$$

where the diffusion step is along the grain boundary region (Coble creep).

Here D is the diffusion coefficient ($m^2 sec^{-1}$), δ is the effective boundary width (m), Ω is the molecular volume ($3.1 \times 10^{-17} m^3$ for Al_2O_3) and G is the grain size.

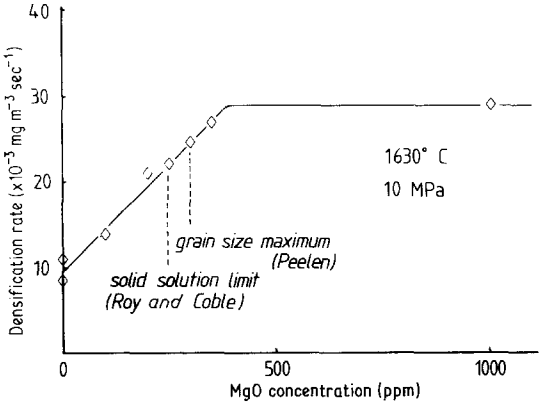

Figure 5 Dependence of the densification rate of Al_2O_3 on the MgO content within the solid solution regime. Other solubility data are included in the figure for comparison.

4.1.2. Grain size dependence

The observation of a grain size exponent of − 2 for the pure Al_2O_3 at low temperature (1475° C) is consistent with control by a lattice diffusion mechanism. At higher temperatures, the grain size dependence for both pure and MgO-doped Al_2O_3 shows mixed behaviour and indicates a shift from lattice control ($\dot{\rho} \propto (GS)^{-2}$) at small grain sizes to grain boundary control ($\dot{\rho} \propto (GS)^{-3}$) at larger grain sizes. This shift can be best explained in terms of a gradual transition from control by Al lattice diffusion at small grain sizes to control by oxygen boundary diffusion at larger grain sizes.

Tracer diffusion studies [28, 29] and diffusional creep experiments [26] in Al_2O_3 suggest that $\delta D_O^b \gg \delta D_{Al}^b$ and $D_{Al}^L \gg D_O^L$ so that four con-

trolling diffusion steps are in principle observable as the grain size is raised, the expected sequence being:

	D^b_{Al}	D^L_{Al}	D^b_O	D^L_O
expected grain size dependence	(−3) →	(−2) →	(−3) →	(−2)

direction of increasing grain size

A gradual change in the grain size exponent from −2 to −3 with increasing grain size as observed in the present data signifies a shift in the process step, in accordance with the above sequence, from D^L_{Al} to D^b_O. Further evidence for a shift in mechanism from Al^{3+} lattice control to O^{2-} boundary control is given by the temperature dependence of the grain size exponent for pure Al_2O_3. At the lower temperature (1475° C) the exponent for undoped Al_2O_3 is −2 consistent with Al^{3+} lattice control. At the higher temperature (1630° C), the grain size exponent shifts to predominantly −3 consistent with control by O^{2-} diffusion along the grain boundaries. The switch in mechanism occurs in this case because the lattice diffusion process has the higher activation energy. According to the data, doping with MgO has a greater effect on aluminium lattice diffusion than it has on oxygen grain boundary diffusion.

4.1.3. Calculated diffusion coefficients

Values for D^L_{Al} and D^b_O may be calculated from the densification data to compare with other values available in the literature. Applying Equation 1 and using Coble's [21] expression for the effective stress, a value of 2×10^{-13} m^2 sec^{-1} was calculated for D^L_{Al} from the densification data for pure Al_2O_3, 1630° C, 1 μm grain size. Other estimates of D^L_{Al} inferred from creep measurements of pure and Fe-doped Al_2O_3, MgO-saturated Al_2O_3 and tracer self-diffusion experiments are listed in Table I for comparison.

The observed value best agrees with the values obtained from the viscous creep of Fe-doped Al_2O_3, obtained under similar stress and temperature conditions.

Using Equation 2, a value of 3×10^{-19} m^3 sec^{-1} was estimated for δD^b_O from the densification data for pure Al_2O_3, 1630° C (using the 10 μ grain size data). Other estimates of D^b_O calculated from the creep of Fe-doped alumina, abnormal grain growth and oxygen self-diffusion are listed in Table II for comparison.

Also included in the table is an estimate of δD^b_{Al}. Two features are noteworthy from the data; first, that the value for δD^b_O is in close agreement with the values estimated by Lessing and Gordon for the creep of Fe-doped alumina and second, that the value of δD^b_O is about two orders of magnitude higher than that of δD^b_{Al} estimated by Cannon and Coble on the basis of the available creep data for MgO-saturated Al_2O_3.

The relationship between the various possible controlling mechanisms can best be illustrated by displaying them on a deformation map; Lessing and Gordon [30] have constructed such maps to illustrate creep deformation mechanisms in iron-doped alumina. An updated map (of T against GS) constructed from the hot pressing data in this study is shown in Fig. 7 for pure Al_2O_3. The input data along with the various assumptions made are shown below:

$$D^L_{Al} = 1.87 \times 10^7 \exp\left(\frac{-578\,\text{kJ mol}^{-1}}{RT}\right) \text{cm}^2\,\text{sec}^{-1};$$

TABLE I Aluminium ion lattice diffusion coefficients

Value of D^L_{Al} at 1630° C (m^2 sec^{-1})	Reference	Comments
2×10^{-13}	This study	Hot pressing, 10 MPa, pure Al_2O_3
9×10^{-13}	Lessing and Gordon [30]	Creep; 5 MPa, Al_2O_3 + 2% Fe
2×10^{-14}	Lessing and Gordon [30]	Creep; 5 MPa, pure Al_2O_3
4×10^{-15}	Cannon and Coble [26]	Creep, MgO-saturated Al_2O_3
3×10^{-16}	Paladino and Kingery [28]	Tracer (extrapolated)
2×10^{-10}	Rossi *et al.* [31]	Intermediate stage hot pressing, pure Al_2O_3 (extrapolated from 1350° C).

TABLE II Boundary diffusion coefficients in Al_2O_3

δD_O^b ($m^3 sec^{-1}$)	Reference	Comments
3×10^{-19}	This study	Hot pressure, pure Al_2O_3, 10 MPa
6×10^{-19}	Lessing and Gordon [30]	Creep, Al_2O_3 + 2% Fe, 5 MPa, oxidizing conditions.
5×10^{-22}	Oishi and Kingery [29]	Self-diffusion
δD_{Al}^b ($m^3 sec^{-1}$)	Cannon and Coble [26]	Creep, MgO saturated Al_2O_3.
2×10^{-21} 2×10^{-21}		

$$\delta D_O^b = 4 \times 10^{-1} \exp\left(\frac{-440\,kJ\,mol^{-1}}{RT}\right) cm^2 sec^{-1};$$

$$\delta D_{Al}^b = 8.6 \times 10^{-4} \exp\left(\frac{-419\,kJ\,mol^{-1}}{RT}\right) cm^2 sec^{-1}.$$

A change in the process step from aluminium ion lattice diffusion to oxygen boundary diffusion is estimated from the data in Fig. 4 (1630° C) to occur at 5 μm. The value of δD_{Al}^b is taken from a review by Cannon and Coble [26]. Activation energies for D_{Al}^L and D_O^b were taken from the data of Cannon and Coble [26] and Lessing and Gordon [30], respectively.

4.1.4. Additive dependence

The results of Fig. 5 show that, in the first instance, MgO increases the densification rate, with a linear dependence on additive content, until the solubility limit is reached; thereupon saturation occurs and the densification rate levels off. The solubility limit at 1630° C, estimated from the data, is ~400 ppm which is in reasonable agreement with other published limits ($\geqslant$ 300 ppm [4] and 250 ppm [24]). Marked on the deformation map is the point at which the effect of MgO has been studied; it may be seen that the dependence of the densification rate on MgO content has been determined in the regime where densification is controlled by Al^{3+} lattice diffusion. The effect of the additive in enhancing densification in the solid solution range can therefore be interpreted as being due to the raising of the Al ion diffusion coefficient.

The calculated dependencies of point defect concentrations in Al_2O_3 on the concentration of added MgO for the two most plausible defect models are shown in Figs 8 and 9. The important feature is that both models can predict a linear increase in the concentration of aluminium interstitial ions ($Al_i^{\cdot\cdot\cdot}$) with MgO content. Accordingly, it is suggested that additions of MgO increase the sintering rate by generating $Al_i^{\cdot\cdot\cdot}$ defects, since $D_{Al} = D_{Al_i^{\cdot\cdot\cdot}}$ ($Al_i^{\cdot\cdot\cdot}$), an argument that is independent of the exact nature of the dominant defect disorder type assumed for pure Al_2O_3. The similarity between the Schottky and Frenkel defect models at high MgO contents presents a major difficulty in determining the dominant defect disorder type in pure Al_2O_3 on the basis of kinetic data.

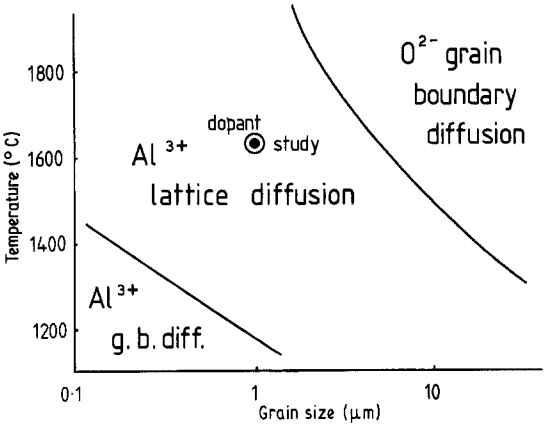

Figure 7 Deformation map constructed for pure Al_2O_3 from the present hot-pressing data and other sources.

4.2. Interpretation of the role of MgO in the sintering of Al_2O_3

There are many varied interpretations and conflicting accounts concerning the role of MgO in the sintering of Al_2O_3. Some causes for these discrepancies have already been outlined in the introduction.

From the present results, it is clear that MgO acts in solution to accelerate the rate of densification during hot pressing; it is also known that MgO is an effective sintering aid in this solid solution region.

In attempting to link these ideas it is useful to used, as a basis, the function of a sintering additive. This function is now widely agreed to be the ability of the additive to prevent abnormal grain growth, i.e. to retain the pores at the grain

boundaries so that the diffusion distances involved in sintering (from the boundaries to the pores) are kept short.

The prevention of abnormal grain growth is achieved if [1]

$$\frac{M_p F_p}{M_b} > F_b - N F_p ,$$

where M_p, M_b and F_p, F_b represent the mobilities of, and forces acting on, the pores and boundaries respectively. N is the pore density at the boundary. Since F_p and F_b are functions of the geometry of the system, the function of the additive is through its effect on the (M_p/M_b) ratio. (Qualitatively, abnormal growth is prevented *either* if M_b is low, i.e. the boundaries are slow-moving, *or* M_p is high, i.e. the pores are capable of rapid movement; under both conditions the dragged pores are able to remain in contact with the boundary.)

Inhibition of boundary migration, M_b, by solute drag as originally proposed by Jorgensen and Westbrook [32], has been questioned for several reasons, namely (i) Auger and X-ray photoelectron spectroscopy (XPS) surface analysis studies do not reveal any significant enhancement of MgO at the grain boundaries in MgO-doped Al_2O_3 [13], (ii) calcium additions, although known to segregate very strongly to the grain boundaries in sintered Al_2O_3 [33], are totally ineffective in aiding densification, and (iii) MgO additions have been observed to produce an increased grain size

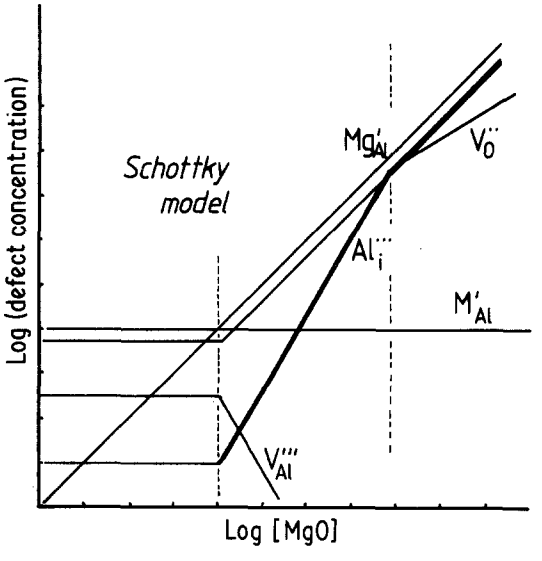

Figure 8 Dependence of point defect concentrations on the MgO content for impure Al_2O_3 (low M^{2+} impurity content) assuming Schottky Disorder in the pure host.

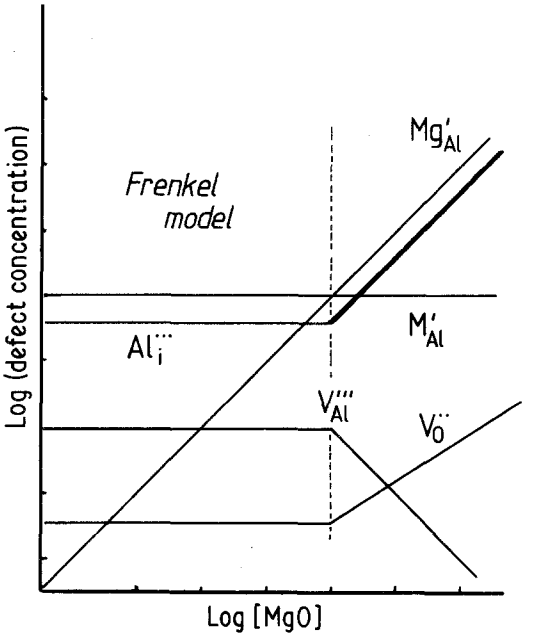

Figure 9 Dependence of point defect concentrations on the MgO content for impure Al_2O_3 (low M^{2+} impurity content) assuming Frenkel Disorder in the pure host.

[4, 17]. These observations are consistent with the view advanced earlier [17] that boundary migration is controlled by the movement of attached pores rather than by impurities segregated at the grain boundaries. Consequently, the essential role of the additive is not seen as lying in its effect on M_b.

Turning to M_p, it has been suggested [1] that the most rapid mechanism for pore movement during sintering is by a process of surface diffusion of atoms from the front wall of the pore to the back, for which

$$M_p = K \frac{D_s}{r^4} ,$$

where K is a constant, D_s a surface diffusion coefficient, and r the pore radius. Thus an interpretation of the function of MgO can be based on either a raising of D_s or a reduction of r; both views have been advanced [34, 17].

The present data show that MgO acts to accelerate the densification rate; consequently, the suggested interpretation for the function of MgO as sintering additive on the basis of the results is that:

(a) MgO raises the aluminium lattice diffusion coefficient by raising the concentration of $Al_i^{\cdot\cdot\cdot}$;

(b) the higher lattice diffusion coefficient increases the rate of pore removal;

(c) at a given stage in microstructural develop-

ment (grain size), pores will be smaller when MgO is present;

(d) the small r greatly increases M_p;

(e) the large M_p prevents separation of the pores from the boundaries and hence eliminates abnormal grain growth.

5. Conclusions

(a) When added in solid solution, MgO is shown to enhance densification during hot-pressing; for the conditions of temperature and particle size used in the experiments, the rate controlling process in densification is believed to be aluminium lattice diffusion. Consequently, MgO additions raise $(D_{Al})_L$; this suggests that $Al_i^{\cdot\cdot\cdot}$ is the controlling defect for aluminium diffusion.

(b) In view of its ability to raise $(D_{Al})_L$, MgO is expected to cause more rapid pore removal during sintering. The consequent reduction in pore size, r, and enhancement of pore mobility, M_p, are seen as important steps in allowing pores to remain attached to moving grain boundaries, and hence in avoiding abnormal grain growth. This interpretation provides a model for the role of MgO as sintering aid in Al_2O_3 within the solid solution regime.

References

1. R. J. BROOK, in "Treatise on Materials Science and Technology 9", edited by F. F. Y. Wang (Academic Press, New York, 1976) pp. 331–64.
2. R. L. COBLE, *J. Appl. Phys.* **32** (1961) 793.
3. I. B. CULTER, *Bull. Amer. Ceram. Soc.* **57** (1978) 316.
4. J. G. J. PEELEN, in "Materials Science Research 10", edited by G. C. Kuczynski (Plenum Press, New York, 1975) p. 443.
5. F. A. KROGER and V. J. VINK, in "Solid State Physics 3", edited by F. Seitz and D. Turnball (Academic Press, New York and London, 1966) pp. 307–435.
6. J. W. CAHN, *Acta Met.* **10** (1962) 789.
7. S. PROCHAZKA and R. M. SCANLAN, *J. Amer. Ceram. Soc.* **58** (1975) 72.
8. W. D. KINGERY and B. FRANCOIS, in "Sintering and Related Phenomena", edited by G. C. Kuczynski, N. A. Hooten and C. F. Gibbon (Gordon and Breach, New York, 1967) pp. 471–98.
9. D. L. JOHNSON, in "Processing of Crystalline Ceramics", Materials Science Research Vol. 11, edited by H. Palmour III, R. F. Davis and T. M. Hare (Plenum Press, New York) p. 137.
10. W. D. KINGERY, *J. Appl. Phys.* **30** (1959) 301.
11. C. ZENER, private communication to C. S. Smith, *Trans. AIME* **175** (1948) 15.
12. W. D. KINGERY, *J. Amer. Ceram. Soc.* **57** (1974) 74.
13. W. C. JOHNSON and D. F. STEIN, *J. Amer. Ceram. Soc.* **58** (1975) 485.
14. O. L. KRIVANEK, M. P. HARMER and R. GEISS, Proceedings of the 9th International Conference on Electron Microscopy, Toronto, Vol. 1 (1978) (Imperial Press, Ontario, 1978) p. 414.
15. E. DI RUPO, T. G. CARRUTHERS and R. J. BROOK, *J. Amer. Ceram. Soc.* **61** (1978) 468.
16. I. W. JONES and L. J. MILES, *Proc. Brit. Ceram. Soc.* **19** (1971) 161.
17. M. P. HARMER, E. W. ROBERTS and R. J. BROOK, *Trans. J. Brit. Ceram. Soc.* **78(1)** (1979) 22.
18. *Idem,* to be published in "Energy and Ceramics" Proceedings of the 4th CIMTEC Meeting, Materials Science Monographs 6 (Elsevier Science Publishers, Oxford, 1980).
19. R. J. WESTON and T. G. CARRUTHERS, *Proc. Brit. Ceram. Soc.* **22** (1973) 197.
20. L. J. BOWEN, R. J. WESTON, T. G. CARRUTHERS and R. J. BROOK, *J. Mater. Sci.* **13** (1978) 341.
21. P. L. FARNSWORTH and R. L. COBLE, *J. Amer. Ceram. Soc.* **49** (1966) 264.
22. W. BEERE, *J. Mater. Sci.* **10** (1975) 1434.
23. R. L. COBLE, in "Sintering and Related Phenomena", edited by G. C. Kuczynski, N. A. Hooten and C. F. Gibbon (Gordon and Breach, New York, 1967) pp. 329–50.
24. S. K. ROY and R. L. COBLE, *J. Amer. Ceram. Soc.* **51** (1968) 1.
25. C. HERRING, *J. Appl. Phys.* **21** (1950) 437.
26. R. M. CANNON and R. L. COBLE in "Deformation of Ceramic Materials", edited by R. C. Bradt and R. E. Tressler (Plenum Press, New York, 1975) p. 61.
27. R. L. COBLE, *J. Appl. Phys.* **41 (12)** (1970) 4798.
28. A. E. PALADINO and W. D. KINGERY, *J. Chem. Phys.* **37 (5)** (1962) 957.
29. Y. OISHI and W. D. KINGERY, *ibid.* **33 (2)** (1960) 480.
30. P. A. LESSING and R. S. GORDON, *J. Mater. Sci.* **12** (1977) 2291.
31. R. C. ROSSI, J. D. BUCH and R. M. FULRATH, *J. Amer. Ceram. Soc.* **53** (1970) 629.
32. P. J. JORGENSEN and J. H. WESTBROOK, *ibid.* 47 (1964) 332.
33. W. C. JOHNSON and R. L. COBLE, *ibid.* **61 (3–4)** (1978) 110.
34. A. H. HEUER, *ibid.* **62 (5–6)** (1979) 317.

Received 14 April and accepted 12 May 1980.